Developmental Cell
Article

Estrogen-Related Receptor β/NR3B2 Controls Epithelial Cell Fate and Endolymph Production by the Stria Vascularis

Jichao Chen[1,5] and Jeremy Nathans[1,2,3,4,*]
[1]Department of Molecular Biology and Genetics
[2]Department of Neuroscience
[3]Department of Ophthalmology
[4]Howard Hughes Medical Institute
Johns Hopkins University School of Medicine, Baltimore, MD 21205, USA
[5]Present address: Department of Biochemistry, Stanford University School of Medicine, Stanford, CA 94305, USA.
*Correspondence: jnathans@jhmi.edu
DOI 10.1016/j.devcel.2007.07.011

SUMMARY

In the mammalian inner ear, endolymph is produced and resorbed by a complex series of epithelia. We show here that estrogen-related receptor β (ERR-β; NR3B2), an orphan nuclear receptor, is specifically expressed in and controls the development of the endolymph-producing cells of the inner ear: the strial marginal cells in the cochlea and the vestibular dark cells in the ampulla and utricle. *Nr3b2*$^{-/-}$ strial marginal cells fail to express multiple ion channel and transporter genes, and they show a partial transformation toward the fate of the immediately adjacent Pendrin-expressing epithelial cells. In genetically mosaic mice, *Nr3b2*$^{-/-}$ strial marginal cells produce secondary alterations in gene expression in the underlying intermediate cells and a local loss of strial capillaries. A systematic comparison of transcripts in the WT versus *Nr3b2*$^{-/-}$ stria vascularis has identified a set of genes that is likely to play a role in the development and/or function of endolymph-producing epithelia.

INTRODUCTION

Auditory and vestibular sensory cells within the inner ear detect sound pressure waves and linear or angular acceleration by sensing the deflection of the hair bundle, an exquisitely sensitive mechanoelectrical transduction device (Hudspeth, 2001). Hair bundle deflection is directly coupled to the opening of cation channels, and the resulting inward flow of cations leads to a graded change in neurotransmitter release onto second-order neurons. The types and numbers of ions that flow into the hair cells are determined by the unusual ionic composition of endolymph, the extracellular fluid that bathes the hair bundles on the apical face of the sensory epithelium, and by the ~80 mV endocochlear potential between endolymph and perilymph, the extracellular fluid that bathes the basal face of the sensory epithelium. Perilymph has an ionic composition that is approximately the same as that of other extracellular fluids (~3.5 mM potassium, ~140 mM sodium, and ~1 mM calcium). By contrast, the composition of endolymph more nearly approximates that of cytosol (~150 mM potassium, ~1 mM sodium, and ~20 nM calcium). This unusual system of extracellular fluid compartments has been a source of fascination and intensive investigation ever since the discovery of the endocochlear potential more than half a century ago (Von Bekesy, 1952).

The epithelial lining of the endolymphatic space includes at least ten distinct cell types that are organized in specialized zones, and several of these cell types are critical for secretion and recycling of endolymph (Anniko, 1988; Santi, 1988; Petit et al., 2001; Wangemann, 2006). In the cochlea, the principal site of endolymph production is the stria vascularis, a multilayered and highly vascularized structure that resides in the lateral wall of the scala media. The major pathway of recycling and secretion of cochlear endolymph involves a flow of potassium ions from perilymph to fibrocytes in the spiral ligament (the outer wall of the cochlea) and then to basal cells, intermediate cells, and marginal cells in the stria vascularis, the last of which releases the potassium into the scala media. Each of these steps is precisely orchestrated by a series of gap junctions, channels, pumps, and transporters, many of which have been molecularly identified (Wangemann, 2006). A similar pathway in the ampulla and utricle involves the vestibular dark cells and the immediately underlying melanin-containing cells, analogs, respectively, of the marginal cells and intermediate cells of the stria vascularis (Wangemann, 1995).

The importance of inner-ear fluid homeostasis is underscored by the large number of hereditary human and/or mouse deafness syndromes caused by defects in this process (Steel, 1995; Petit et al., 2001; Peters et al., 2004; Wangemann, 2006). Monogenic auditory and/or vestibular defects (the latter are rare in humans but are common in the mouse) can be caused by mutations in genes encoding the fibrocyte-basal cell gap junction channel subunits GJB2 and GJB6 (Connexins 26 and 30), the

intermediate cell potassium channel KCNJ10, the marginal cell Na-K-2Cl cotransporter SLC12A2, the marginal cell potassium channel subunits KCNQ1 and KCNE1, and the spindle cell chloride-bicarbonate exchanger Pendrin/SLC26A4 (Vetter et al., 1996; Everett et al., 1997; Delpire et al., 1999; Dixon et al., 1999; Flagella et al., 1999; Lee et al., 2000; Letts et al., 2000; Casimiro et al., 2001; Marcus et al., 2002). Other nongenetic or mixed genetic-environmental disorders of hearing and balance may also involve defects in fluid homeostasis. For example, Meniere's disease, an adult-onset disorder characterized by hearing loss, tinnitus, and episodic attacks of vertigo, is associated with enlargement of the endolymphatic space ("endolymphatic hydrops"), which suggests a defect in endolymph production and/or resorption (Paparella and Djalilian, 2002; Gates, 2006).

In the present paper, we show that a nuclear receptor, estrogen-related receptor β (ERR-β; NR3B2), controls the expression of multiple ion channel and transporter genes in strial marginal cells and vestibular dark cells. In the absence of NR3B2, these cells are partially converted to the developmental fate of the immediately adjacent epithelial cells. Interestingly, in the stria vascularis, this developmental switch in the superficial marginal cells affects the pattern of gene expression in the underlying intermediate cells. These experiments provide a window into the developmental logic that governs the generation of complex epithelia involved in inner-ear fluid homeostasis. The experiments reported here also suggest that therapies based on the modulation of inner-ear transcriptional regulatory networks might be used to treat some disorders of hearing and balance.

RESULTS

Auditory and Vestibular Defects in Postnatal *Nr3b2* Mutants

Nr3b2 null embryos die at midgestation as a result of placental abnormalities (Luo et al., 1997). To circumvent this lethal phenotype, we generated an *Nr3b2* conditional allele with *loxP* sites flanking the second exon ($Nr3b2^{CKO}$; Figure 1A). This exon contains the initiator methionine codon and encodes the N-terminal 132 amino acids of NR3B2, including part of the DNA-binding domain; we presume that its deletion inactivates NR3B2 function. Consistent with that supposition, no $Nr3b2^{-/-}$ progeny were obtained in more than ten litters from $Nr3b2^{+/-}$ parents in which the $Nr3b2^{-}$ allele was derived from the $Nr3b2^{CKO}$ allele by Cre excision of exon 2. To obtain viable *Nr3b2* mutant progeny, exon 2 was excised by Cre recombinase expressed from a paternally inherited *Sox2-cre* transgene, which efficiently recombines *loxP* targets in embryonic, but not extraembryonic, tissues (Hayashi et al., 2002, 2003). The resulting $Nr3b2^{CKO/-}$*;Sox2-cre* mice are born and survive to adulthood in the expected Mendelian proportions, and their constituent cells appear to be uniformly $Nr3b2^{-/-}$, as judged by Southern blot hybridization (Figure 1B).

$Nr3b2^{CKO/-}$*;Sox2-cre* mice exhibit head bobbing beginning at several weeks of age, and as adults they spin or run in circles. Mitsunaga et al. (2004) reported a similar observation in a study of germ cell defects in $Nr3b2^{-/-}$ mice that had been generated by tetraploid embryo fusion. In the mouse, circling behavior is a classic sign of defective vestibular function (Steel, 1995), suggesting the possibility that hearing might also be impaired. Indeed, $Nr3b2^{CKO/-}$*;Sox2-cre* mice have no auditory startle reflex, and auditory brainstem responses (ABRs) reveal a threshold in excess of 100 dB sound pressure level (SPL) (Figure 1C). In keeping with these observations, northern blot hybridization with the *Nr3b2* exon 2 probe shows that this gene is expressed in the WT inner ear (Figure 1B). As expected, the exon 2 hybridization signal is absent in the $Nr3b2^{CKO/-}$*;Sox2-cre* inner ear.

Gross examination of dissected $Nr3b2^{CKO/-}$*;Sox2-cre* temporal bones showed normal inner-ear morphology, except for narrowing of the membranous labyrinths of the three semicircular canals and flattening of the ampullae (Figure 1D). In cross-sections of the $Nr3b2^{CKO/-}$*;Sox2-cre* cochlea, the scala media was reduced in volume at postnatal day (P)4 and had collapsed entirely by P7 (Figure 1E). These vestibular and cochlear phenotypes are indicative of diminished endolymph production, and they have been observed previously in mice with mutations in ion channels or transporters that are expressed in the endolymph-producing cells of the stria vascularis and in the analogous secretory epithelia of the vestibular organs (Vetter et al., 1996; Delpire et al., 1999; Dixon et al., 1999; Flagella et al., 1999; Lee et al., 2000; Letts et al., 2000; Casimiro et al., 2001).

Nr3b2 Is Expressed Specifically in the Endolymph-Secreting Strial Marginal Cells and Vestibular Dark Cells

To identify the cells in the inner ear that express *Nr3b2*, we localized *Nr3b2* transcripts by in situ hybridization and NR3B2 protein by immunostaining with affinity-purified antibodies raised against the divergent linker region (amino acids 186–237; Figure 2). In the P3 cochlea, *Nr3b2* transcripts are found exclusively in the marginal cells, the apical monolayer of cells within the stria vascularis that directly contacts the endolymph (Figure 2A). In the P3 crista ampullaris and utricle, *Nr3b2* transcripts are found only in the analogous vestibular dark cells.

Immunostaining at P3 shows that NR3B2 is localized to a monolayer of apical nuclei that corresponds to the endolymph-secreting cells, as determined by coexpression of the potassium channel subunit KCNQ1 (Figure 2B). In both the cochlea and the vestibular organs, strial marginal cell and vestibular dark cell epithelia have precise and well-demarcated borders: in the cochlea, this epithelium extends from ~2–3 cells above the spiral prominence to ~1–2 cells below the insertion of Reissner's membrane; in the ampullae it extends laterally, beginning just beneath a notch near the base of the cristae (Anniko, 1988; Santi, 1988). Interestingly, the loss of NR3B2 immunostaining in the $Nr3b2^{CKO/-}$*;Sox2-cre* inner ear results in

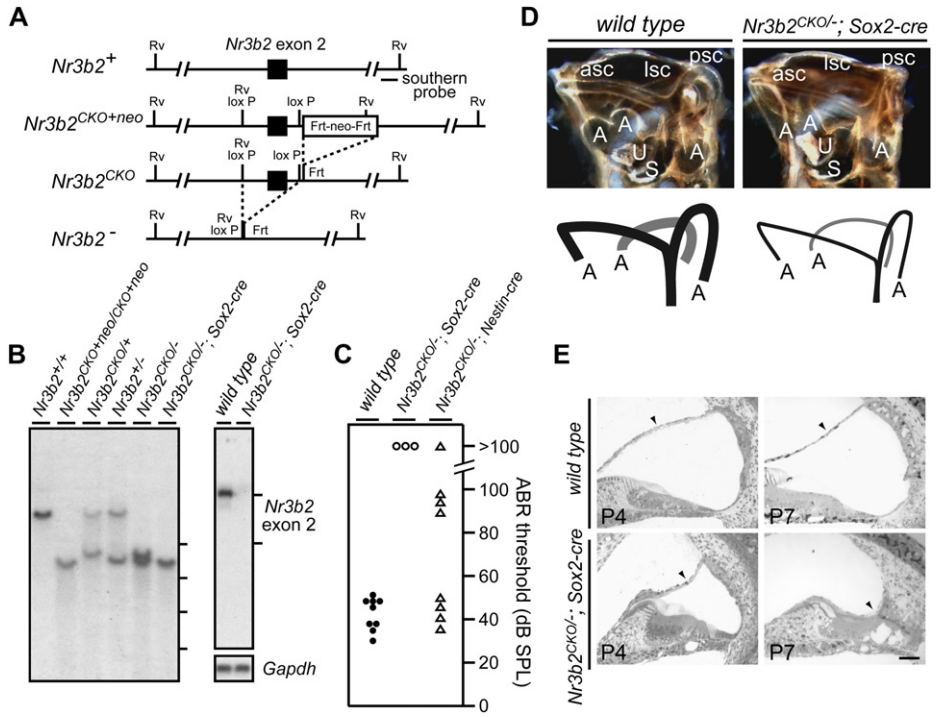

Figure 1. Conditional Loss of *Nr3b2* Causes Deafness and Diminished Endolymphatic Fluid Volume

(A) Genomic structure near *Nr3b2* exon 2, which contains the initiator methionine codon. Top to bottom: WT *Nr3b2* showing the location of the Southern blot probe (*Nr3b2*$^{+}$); the initial gene-targeting product in which exon 2 is flanked by *loxP* sites and is followed by a Frt-flanked *PGK-neo* (*Nr3b2*$^{CKO+neo}$); the targeted allele following Flp-mediated excision of the *neo* cassette (*Nr3b2*^{CKO}); the *Nr3b2* loss-of-function allele obtained by Cre-mediated excision of exon 2 (*Nr3b2*$^{-}$). Dotted lines show site-specific recombination events. Rv, EcoR V sites.

(B) Left, Southern blot hybridization of EcoR V-digested genomic DNA showing hybridization patterns for the four alleles illustrated in (A). Molecular weight markers are (from top to bottom): 12, 10, 8, and 6 kb. Right, northern blot of RNA from WT and *Nr3b2*$^{CKO/-}$*;Sox2-cre* P3 inner ears probed with *Nr3b2* exon 2. The mobilities of 18S and 28S rRNAs are indicated by lines to the right of the blot. Hybridization of *Gapdh* (bottom) demonstrates equal loading of RNA.

(C) Auditory brainstem response thresholds of (left to right) WT, *Nr3b2*$^{CKO/-}$*;Sox2-cre*, and *Nr3b2*$^{CKO/-}$*;Nestin-cre* mosaics, between 1 and 3 months of age. *Nr3b2*$^{CKO/-}$*;Sox2-cre* mutants show no response at any stimulus level, including the highest level of 100 dB SPL. *Nr3b2*$^{CKO/-}$*;Nestin-cre* mosaics show wide individual variation in sensitivity.

(D) Thinning of the membranous labyrinths of the semicircular canals in *Nr3b2*$^{CKO/-}$*;Sox2-cre* mutants. The vestibular system is otherwise grossly normal. A diagram of the three semicircular canals is shown below. A, ampulla; U, utricle; S, saccule; asc, lsc, and psc, anterior, lateral, and posterior semicircular canals, respectively.

(E) Cross-section through the cochlea showing the collapse of the scala media during the first postnatal week (P4, left, and P7, right) in *Nr3b2*$^{CKO/-}$*;Sox2-cre* mutants. Reissner's membrane is indicated by an arrowhead. The scale bar is 200 μm.

a concomitant loss of KCNQ1 (Figure 2B). KCNQ1 and KCNE1 coassemble to form the apical I_{SK} channel in the strial marginal cells and vestibular dark cells, and targeted deletion of either subunit in the mouse causes a decrease in potassium secretion into the endolymph and collapse of the endolymphatic space (Vetter et al., 1996; Lee et al., 2000; Letts et al., 2000; Casimiro et al., 2001). Sensorineural deafness and endolymphatic collapse are also seen in humans with mutations in these genes (Jervell and Lange-Nielson syndrome) (Friedmann et al., 1966; Schulze-Bahr et al., 1997; Wang et al., 2002).

Reduction in the Expression of Multiple Channels and Transporters in *Nr3b2*$^{-/-}$ Marginal Cells

Given the presumptive role of NR3B2 as a transcriptional regulator, it seemed plausible that the absence of KCNQ1 protein in the *Nr3b2*$^{CKO-}$*;Sox2-cre* inner ear might reflect a corresponding absence of *Kcnq1* transcripts. It also seemed plausible that transcripts encoding other strial marginal cell and vestibular dark cell channels or transporters might be affected. In situ hybridization to sections through the P3 cochlea and northern blots of RNA prepared from the dissected ~P4 organ of Corti and lateral wall of the cochlea (the latter containing the stria vascularis; see Figure 7A) shows a complete or nearly complete loss of transcripts encoding KCNQ1, KCNE1, and ATP1B2 (one subunit of the Na/K ATPase), and a partial loss of transcripts encoding ATP1A1 (a second Na/K ATPase subunit) in the *Nr3b2*$^{CKO/-}$*;Sox2-cre* lateral wall (Figure 3). In the WT cochlea, *Slc12a2* transcripts are present in both the marginal cells of the stria vascularis and the organ of Corti; in the *Nr3b2*$^{CKO/-}$*;Sox2-cre* cochlea, they are substantially reduced in the former, but not the latter. Interestingly, in situ hybridization with a probe

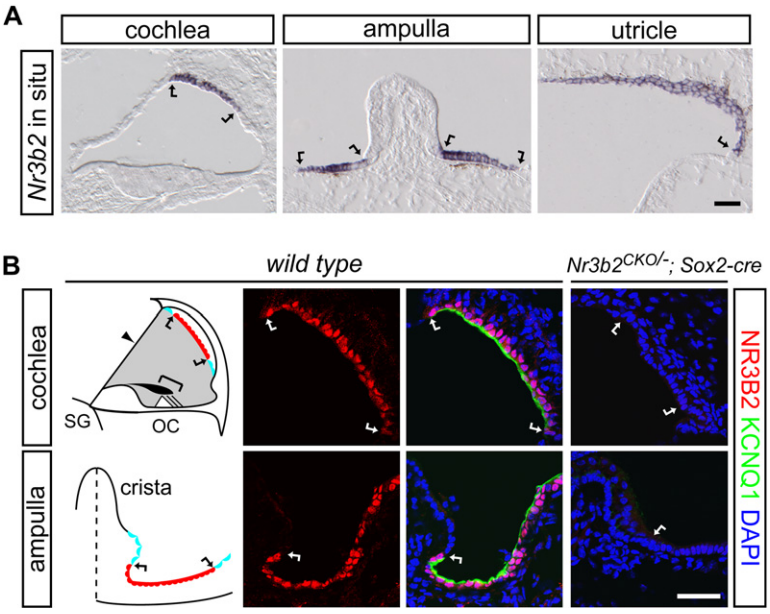

Figure 2. *Nr3b2* Is Expressed Specifically in the Apical Epithelial Cells Responsible for Endolymph Production in the Auditory and Vestibular Systems

(A) In situ hybridization in the WT P3 inner ear localizes *Nr3b2* transcripts (purple) to the marginal cells of the stria vascularis (left) and the analogous epithelial zones flanking the crista ampullaris (center) and within the utricle (right). Bent arrows indicate the extent of these zones in this and subsequent images. In the vestibular organs, a fine layer of melanin pigment (brown) is seen immediately beneath the hybridizing epithelial cells. The scale bar is 40 μm.

(B) Immunolocalization of NR3B2 and KCNQ1 within the same endolymph-producing epithelial cells in the WT cochlea and ampulla at P3. The schematic diagrams to the left show the location and orientation of these and all subsequent cross-sectional images of the cochlea and ampulla. The arrowhead indicates Reissner's membrane. The arrows demarcate the epithelia (in red) comprising an endolymph-producing strial marginal cells (in the cochlea) or a vestibular dark cells (in the ampulla). Epithelial cells shown in pale blue express Pendrin. The bracket indicates the organ of Corti. SG, spiral ganglion; OC, organ of Corti. Immunofluorecent images show that, in the WT, NR3B2 localizes to the nucleus and KCNQ1 localizes to the apical plasma membrane (left panels); both are absent from the *Nr3b2*$^{CKO/-}$*;Sox2-cre* inner ear (right panels). The scale bar is 40 μm.

encompassing the complete *Nr3b2*-coding region (Figure 3, top panel) shows continued accumulation of this internally deleted transcript in *Nr3b2*$^{CKO/-}$*;Sox2-cre* marginal cells, indicating that these cells remain at least partly committed to an original cell fate that includes *Nr3b2* expression. Consistent with the excision of the 410 bases derived from exon 2, close inspection of the northern blot shows a small increase in electrophoretic mobility of the *Nr3b2* transcripts in the *Nr3b2*$^{CKO/-}$*;Sox2-cre* sample. Taken together, these data imply that NR3B2 positively regulates (directly or indirectly) multiple channel and transporter genes, but not its own gene.

As a test of the cell autonomy (or lack thereof) of the phenotypes associated with loss of *Nr3b2*, we took advantage of the serendipitous observation that site-specific recombination of the *Nr3b2*^{CKO} allele by the Cre recombinase produced from a *Nestin-cre* transgene (Tronche et al., 1999) occurs in roughly half of the marginal and vestibular dark cells, that the recombined cells are finely intermingled with cells that are not recombined, and that the mosaicism is relatively stable in postnatal mice. In keeping with this mosaicism, *Nr3b2*$^{CKO/-}$*;Nestin-cre* mice exhibit variably elevated ABRs between 1 and 3 months of age (Figure 1C). However, none show head bobbing or circling.

In the *Nr3b2*$^{CKO/-}$*;Nestin-cre* inner ear, KCNQ1 is lost from *Nr3b2*$^{-/-}$ strial marginal cells, but it continues to accumulate in the apical plasma membrane in immediately adjacent unrecombined *Nr3b2*$^{CKO/-}$ marginal cells (Figure 4A). A similar pattern is seen for SLC12A2 in the marginal cell basolateral membrane (Figure 4B). We note that the complete or nearly complete absence of SLC12A2 immunoreactivity in marginal cells that are genotypically *Nr3b2*$^{-/-}$ suggests either that the in situ and RNA blot hybridizations in Figure 3 underestimate the extent to which *Slc12a2* transcript abundance is controlled by NR3B2, or that the stable accumulation of SLC12A2 depends on other proteins that are controlled by NR3B2. These observations indicate essentially complete cell autonomy of NR3B2 function among marginal cells; similar observations were made with vestibular dark cells (data not shown).

Local Influence of *Nr3b2*$^{-/-}$ Marginal Cells on Intermediate Cells and Intraepithelial Capillaries

We next asked whether loss of *Nr3b2* causes nonautonomous effects in cells that do not normally express *Nr3b2*. In the stria vascularis, the basal plasma membrane of the marginal cells is highly convoluted and is in intimate contact with the correspondingly convoluted membrane of the pigmented intermediate cells (Santi, 1988; Wangemann, 2006). Intermediate cells are connected via gap junctions to the underlying basal cells, which are connected to one another and to the lateral wall fibrocytes by additional gap junctions. A dense plexus of intraepithelial capillaries resides within the interfacial zone between marginal cells and intermediate cells. In the secretory epithelia of the crista ampullaris and utricle, there is a similar arrangement of apical epithelial cells (the vestibular dark cells) above a layer of pigmented cells (Anniko, 1988; Wangemann, 1995).

In an initial assessment of intermediate and basal cell viability and differentiation, we found that in the *Nr3b2*$^{CKO/-}$*;Sox2-cre* stria vasularis, transcripts coding for lysine-deficient protein kinase 4 (WNK4) (Kahle et al., 2004), a basal cell marker, were greatly reduced at P3

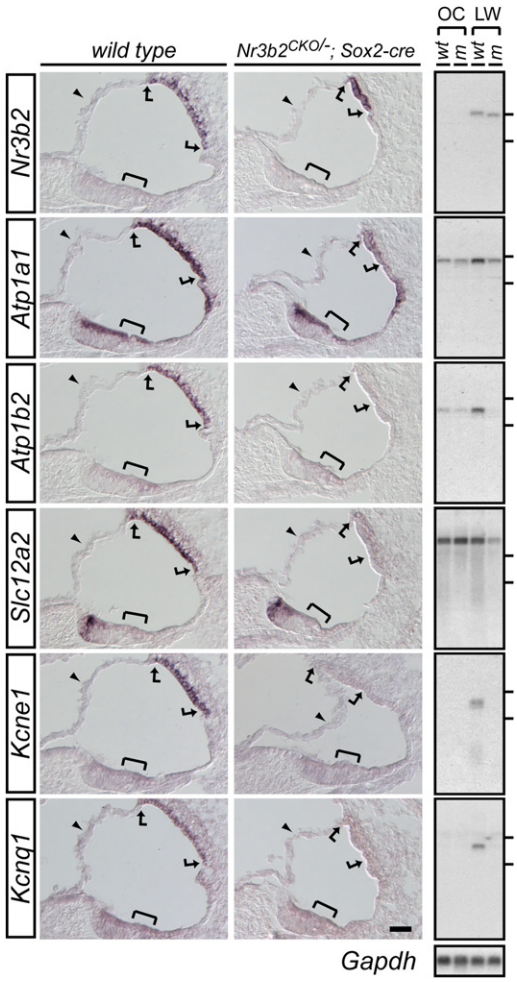

Figure 3. Downregulation of Multiple Ion Channel and Transporter Transcripts in Marginal Cells of the *Nr3b2*$^{CKO/-}$; *Sox2-cre* Stria Vascularis

In situ hybridization of P3 cochleas (left) and northern blot hybridization of dissected ~P4 cochlea RNA (right). OC, organ of Corti; LW, lateral wall (including the stria vascularis; see Figure 7 for details of the dissection); m, *Nr3b2*$^{CKO/-}$;*Sox2-cre* mutant. The *Nr3b2* hybridization probe encompasses the full coding region (exons 2–7), and its hybridization reveals the accumulation of transcripts derived from the mutant *Nr3b2* gene lacking exon 2. Careful inspection of the northern blot reveals the increased mobility of the mutant *Nr3b2* transcript relative to the WT *Nr3b2* transcript, consistent with the loss of the 410 bases corresponding to exon 2. In the marginal cell epithelium of the *Nr3b2*$^{CKO/-}$;*Sox2-cre* mutant, *Atp1b2*, *Kcne1*, and *Kcnq1* transcripts are completely or almost completely absent, and *Atp1a1* and *Slc12a2* transcripts show a partial decrement. The mobilities of 18S and 28S rRNAs are indicated by lines to the right of the blots. Hybridization of *Gapdh* (bottom) demonstrates equal loading of RNA. The scale bar is 40 μm.

(Figure 4C), and transcripts coding for L-dopachrome tautomerase (DCT), an enzyme involved in melanin biosynthesis in intermediate cells, were progressively lost between P3 and P21 (Figure 4D). Prostaglandin D2 synthase (PTGDS) transcripts are present in marginal, intermediate, and basal cells in the WT stria vascularis, but are confined to intermediate cells in the *Nr3b2*$^{CKO/-}$;*Sox2-cre* stria vascularis; their abundance declines with age (data not shown; changes in *Wnk4* and *Ptgds* transcript levels were initially discovered by microarray hybridization as described below). KCNJ10 potassium channels, which normally reside in the plasma membrane convolutions of intermediate cells (Ando and Takeuchi, 1999), are lost in the *Nr3b2*$^{CKO/-}$;*Sox2-cre* stria vascularis (data not shown). Interestingly, this loss appears to reflect local interactions between marginal and intermediate cells because, in mosaic *Nr3b2*$^{CKO/-}$;*Nestin-cre* mice, the loss of KCNJ10 is confined to those intermediate cells in close contact with *Nr3b2*$^{-/-}$ marginal cells (Figure 4E).

The uniform loss of *Nr3b2* from all of the marginal cells in the *Nr3b2*$^{CKO/-}$;*Sox2-cre* stria vascularis also results in a complete absence of intraepithelial capillaries at P3 (visualized with DIC optics and anti-PECAM immunostaining; Figures 4C and 5A). This is not a general consequence of physiologic dysfunction within the stria vascularis because capillary loss is not observed with targeted deletion of *Kcne1*, which abolishes endolymphatic potassium secretion and leads to a complete collapse of the scala media (Vetter et al., 1996). Intraepithelial capillaries are also surprisingly resistant to the loss of intermediate cell contacts, since the capillaries are still present in the thinned stria vascularis of mice homozygous for the *spotted lethal* allele of the gene encoding Endothelin receptor B (*Ednrb*$^{s-l/s-l}$), a null allele in which the neural crest-derived intermediate cells fail to migrate to the stria vascularis (Figure 5A) (Lane, 1966; Tachibana et al., 2003). As described above for KCNJ10 immunostaining, capillary loss is determined by the *Nr3b2* genotype of the immediately overlying marginal cells. In flat mounts of the mosaic *Nr3b2*$^{CKO/-}$;*Nestin-cre* stria vascularis at P6, a good correspondence is seen between the spatial distribution of *Nr3b2*$^{-/-}$ marginal cells (visualized with anti-KCNQ1) and regions of capillary loss (visualized with GS-lectin; Figure 5B). Transmission electron microscopic comparison of WT and *Nr3b2*$^{CKO/-}$;*Sox2-cre* stria vascularis confirms the loss of capillaries at P4 in the mutant inner ear, the earliest time point examined, and also shows a progressive disorganization of basal, intermediate, and marginal cells between P4 and P30 (data not shown).

Partial Conversion of *Nr3b2*$^{-/-}$ Strial Marginal Cell and Vestibular Dark Cell Fates

Within the stria vascularis, the monolayer of marginal cells is flanked by epithelial stripes 1–2 cells wide consisting of spindle cells that express the chloride-bicarbonate exchanger Pendrin/SLC26A4 (Figure 6B) (Wangemann et al., 2004). Additional Pendrin-expressing epithelial cells populate the spiral prominence and outer sulcus, regions adjacent to the stria on the side opposite the point of insertion of Reissner's membrane. In the ampulla, Pendrin-expressing cells populate the transitional epithelium, which resides between the vestibular dark cells and the neurosensory epithelium of the crista (Figure 6B).

The initial clue that loss of *Nr3b2* was associated not only with loss of marginal cell-specific gene expression,

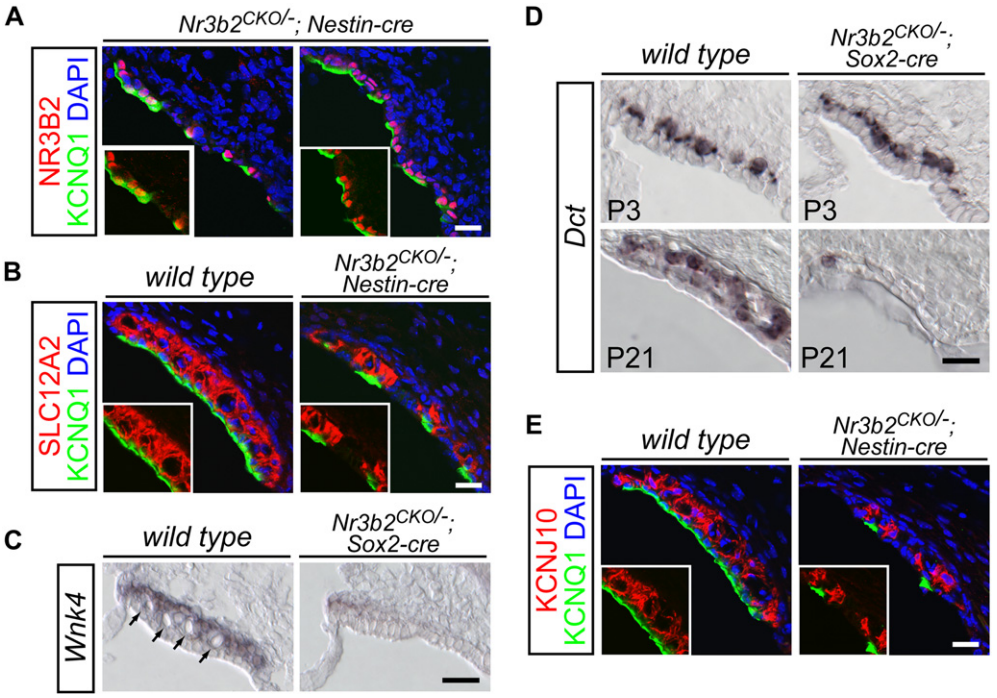

Figure 4. *Nr3b2* Functions Cell Autonomously in Strial Marginal Cells and Causes Secondary Defects in the Immediately Adjacent Intermediate Cells

(A) Mosaic loss of *Nr3b2* induced by a *Nestin-cre* transgene leads to the loss of the apical potassium channel KCNQ1 only in those marginal cells that lack NR3B2. Two different regions of the same mosaic P3 cochlea are shown. Inserts in this figure and in Figure 6 show a part of the immunostained region without the DAPI channel for clearer visualization of NR3B2 immunostaining in nuclei.

(B) Mosaic loss of *Nr3b2* leads to the loss of SLC12A2, a basolateral membrane-specific exchanger, only in those marginal cells that lack NR3B2. WT and mosaic *Nr3b2* mutant stria are shown at P14.

(C) In situ hybridization reveals the loss of *Wnk4* transcripts in basal cells in the *Nr3b2* mutant stria vascularis at P3. In the WT section (left), the arrows indicate intraepithelial capillaries lying between the intermediate cells and the marginal cells.

(D) Progressive loss of *L-dopachrome tautomerase* (*Dct*) transcripts, encoding a melanin biosynthetic enzyme and intermediate cell marker, in the $Nr3b2^{CKO/-}$;*Sox2-cre* stria vascularis. *Dct* transcript levels are unaffected at P3 (upper panel), but progressively decline so that only a single *Dct*-expressing cell remains at P21.

(E) Mosaic loss of Nr3b2 leads to the loss of KCNJ10, a potassium channel that localizes to the face of the intermediate cells in contact with the overlying marginal cells. Only those intermediate cells that reside adjacent to $Nr3b2^{-/-}$ marginal cells (visualized by immunostaining for KCNQ1; see [A]) lack KCNJ10. WT and mosaic *Nr3b2* mutant stria are shown at P14.

Scale bars for all panels are 20 μm.

but with a partial conversion of marginal cell fate, came from immunostaining with sc-20475, a commercial antiserum purported to react with WNK4. Although sc-20475 shows no detectable staining of basal cells, the expected location of WNK4 based on the localization of *Wnk4* transcripts (Figure 4C), we made the serendipitous observation that sc-20475 crossreacts with an antigen in the spindle cells of the stria vascularis, the epithelial cells of the spiral prominence, and Reissner's membrane (Figures 6A and 6B). The crossreacting antigen is also localized to the transitional epithelial cells of the ampulla (Figures 6A and 6B). Thus, in each of these locations, cells that express Pendrin also express the sc-20475 antigen.

Immunostaining of $Nr3b2^{CKO/-}$;*Sox2-cre* or mosaic $Nr3b2^{CKO/-}$;*Nestin-cre* inner ears shows that the sc-20475 antigen is expressed in $Nr3b2^{-/-}$ strial marginal cells and vestibular dark cells at a level comparable to its normal level of expression in the flanking epithelia (Figures 6A and 6B). A similar analysis with anti-Pendrin antibodies shows Pendrin accumulation in some, but not all, of the $Nr3b2^{-/-}$ strial marginal cells, but no Pendrin accumulation in the $Nr3b2^{-/-}$ vestibular dark cells (Figures 6B and 6C). Among the $Nr3b2^{-/-}$ marginal cells, there appears to be a spatial asymmetry in *Pendrin* expression such that cells within the epithelium that are closest to Reissner's membrane have a lower probability of converting to a *Pendrin*-expressing fate. In contrast, subcortical actin bundles, structures that distinguish marginal cells from their epithelial neighbors, are lost from all $Nr3b2^{-/-}$ cells (Figure 6C). In summary, the accumulation of the sc-20475 antigen and the loss of subcortical actin in all $Nr3b2^{-/-}$ marginal and vestibular dark cells, and the accumulation of Pendrin in some of these cells, indicates a partial conversion of $Nr3b2^{-/-}$ cells to the developmental fate of the immediately neighboring Pendrin-expressing cells. However, the continued transcription of the exon

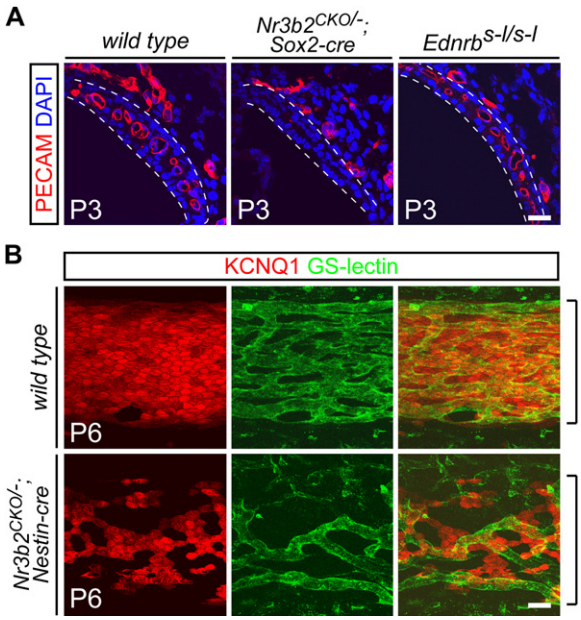

Figure 5. Loss of *Nr3b2* in Strial Marginal Cells Leads to the Localized Loss of Intraepithelial Capillaries

(A) Capillaries visualized by PECAM staining in the P3 stria vascularis. The left and right dashed lines demarcate, respectively, the apical and basal faces of the stria vascularis. A dense capillary plexus is present in the WT and in the *Ednrb*$^{s\text{-}l/s\text{-}l}$ stria, but is missing in the *Nr3b2*$^{CKO/-}$*;Sox2-cre* mutant. The scale bar is 20 μm.

(B) Flatmounts of P6 WT and mosaic *Nr3b2*$^{CKO/-}$*;Nestin-cre* stria vascularis showing intraepithelial capillaries (visualized with GS-lectin) and unrecombined (i.e., phenotypically WT) marginal cells (visualized by immunostaining for KCNQ1). In the *Nr3b2* mosaic, capillaries are lost from regions in which the overlying marginal cells lack KCNQ1 (i.e., *Nr3b2*$^{-/-}$ cells). The spiral prominence is at the bottom of each panel and the insertion of Reissner's membrane is at the top. The vertical brackets to the right of the panels demarcate the extent of the stria vascularis. The scale bar is 20 μm.

2-deleted *Nr3b2* gene in *Nr3b2*$^{-/-}$ strial marginal cells (Figure 3) implies that these cells have retained some of their original properties. The presence of the exon 2-deleted *Nr3b2* transcript in these cells also argues against the trivial possibility that *Nr3b2*$^{-/-}$ marginal cells were simply lost and replaced by Pendrin-expressing cells that migrated across the epithelial surface.

Systematic Analysis of Changes in Gene Expression in the *Nr3b2*$^{-/-}$ Stria Vascularis

The complete or nearly complete absence of various transcripts in each of the stria vascularis cell types in the *Nr3b2*$^{CKO/-}$*;Sox2-cre* cochlea suggests that a systematic analysis of changes in transcript abundance should reveal a set of genes that is relevant to the structure and function of these cells and to the pathophysiology of diseases associated with defects in endolymph homeostasis. For this analysis, we performed three independent sets of dissections of the lateral wall region from WT and *Nr3b2*$^{CKO/-}$*;Sox2-cre* cochleas between P3 and P5, and we compared transcript levels by microarray hybridization (Figures 7A and 7B) (GEO accession number GSE8434). Organ of Corti-enriched transcripts were identified in a separate microarray hybridization to monitor any contamination with this tissue during the lateral wall dissection.

As shown in Figure 7B and Table S1 (see the Supplemental Data available with this article online), with loss of *Nr3b2* a small number of transcripts show a statistically significant decrease in abundance, and an even smaller number show an increase in abundance. Several transcripts that appear to increase in abundance in the *Nr3b2*$^{CKO/-}$*;Sox2-cre* lateral wall, but with statistically insignificant P values, were found to be enriched in the organ of Corti (green squares in Figure 7B); we suspect that these were present in a subset of the lateral wall preparations as dissection artifacts. Among the transcripts exhibiting a >2-fold decrease in abundance in the *Nr3b2*$^{CKO/-}$*;Sox2-cre* lateral wall microarray data set, we have tested eight by northern blot (*Kcne1*, *Aldh1a2*, *Rspo3*, *Ptgds*, *Atp1b2*, *Slc12a2*, *Kcnq1*, and *Wnk4*; red triangles in Figure 7B) and confirmed the decrease in abundance in each case (Figures 3 and 7C). While many of the downregulated transcripts encode transporters or channels that were previously known to be present in the stria vascularis, other differentially regulated transcripts—such as those encoding PTGDS, R-spondin homolog 3, tachkinin receptor 3, aldehyde dehydrogenase 1A2, and a SLIT- and NTRK-like family member—hint at intriguing and unsuspected aspects of inner-ear structure, physiology, and disease.

DISCUSSION

The experiments described above define an essential role for NR3B2 in controlling the development of endolymph-producing epithelia within the inner ear. They also reveal a complex interrelationship among the epithelial, subepithelial, and vascular cells that make up the stria vascularis (Figure 8). In particular, perturbations in the differentiation state of the marginal cells were shown to alter the underlying intermediate, basal, and vascular cells. Finally, by systematically analyzing changes in transcript abundance by microarray, northern blot, and in situ hybridization, we have identified a set of genes that is likely to be of central importance to the development and/or function of endolymph-producing epithelia. In the paragraphs below, we discuss the relevance of these findings to inner-ear development, the control of cell fate decisions by nuclear receptors, and human disorders of hearing and balance.

Transcription Factors, Positional Information, and Cell-Cell Interactions in Inner-Ear Development

Most of the inner-ear transcription factors identified thus far—including *Tbx1*, *Six1*, *Eya1*, *Pax2*, and *Fkh10*—function early in development, and their mutation leads to gross disruptions of inner-ear morphology (Hulander et al., 1998; Zheng et al., 2003; Burton et al., 2004; Ozaki et al., 2004; Moraes et al., 2005; Zou et al., 2006). A smaller number of transcription factors have been identified that function in postmitotic auditory and vestibular sensory

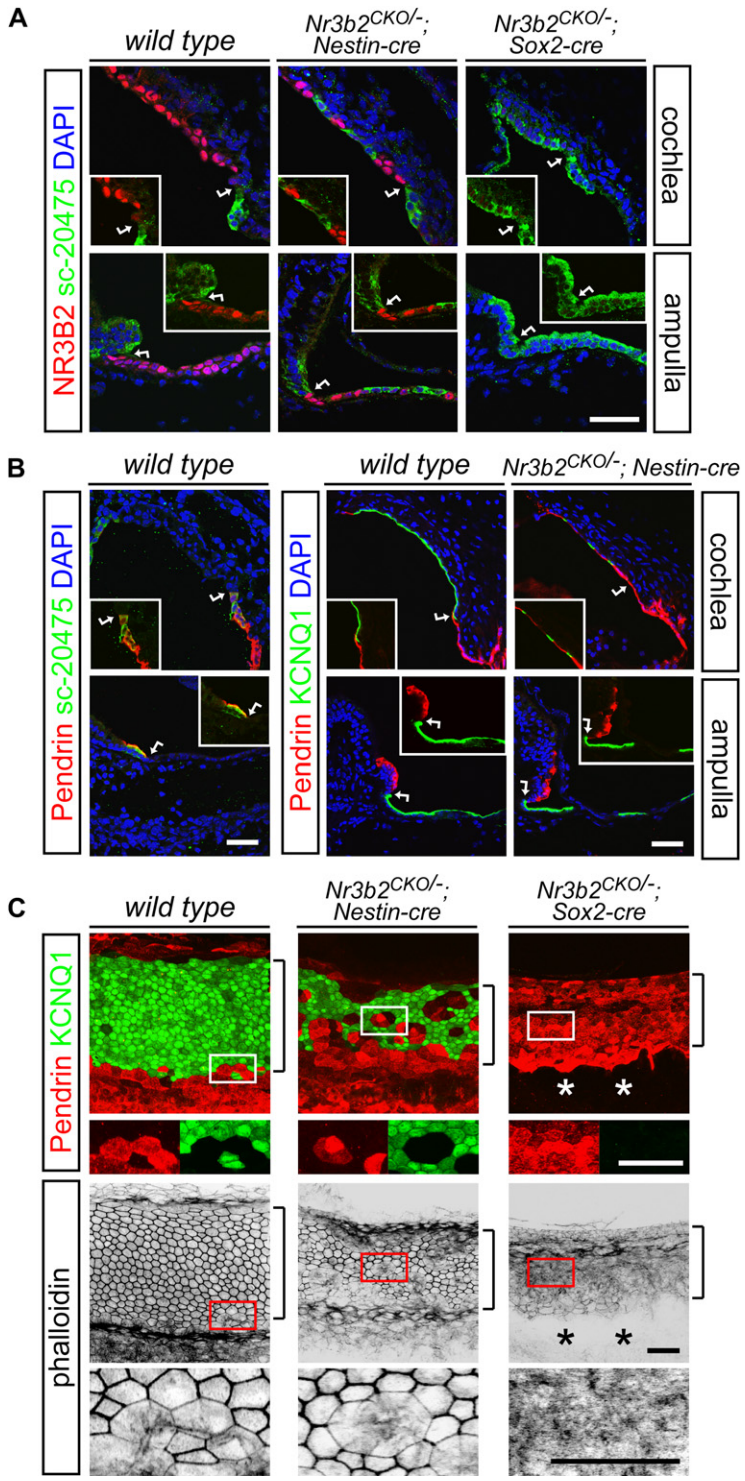

Figure 6. Transdifferentiation of *Nr3b2* Mutant Vestibular Dark Cells and Strial Marginal Cells

(A) At P3, antiserum sc-20475 reveals an intracellular antigen that is confined to epithelial cells adjacent to the endolymph-producing vestibular dark cells in the ampulla and strial marginal cells in the cochlea (left panels). Mosaic or uniform loss of *Nr3b2* (center and right panels, respectively) leads to expression of the sc-20475 antigen in $Nr3b2^{-/-}$ vestibular dark cells and strial marginal cells.

(B) The expression of Pendrin largely coincides with the expression of the sc-20475 antigen in the WT P6 cochlea and ampulla (left panels). At P14, mosaic loss of *Nr3b2* leads to expression of Pendrin in many, but not all, $Nr3b2^{-/-}$ marginal cells, but does not lead to Pendrin expression in $Nr3b2^{-/-}$ vestibular dark cells (right panels). The loss of *Nr3b2* is revealed by the absence of KNCQ1.

(C) Flatmounts of the stria vascularis at P14 showing a graded and heterogeous expansion of Pendrin expression and cytoskeletal reorganization among *Nr3b2* mutant marginal cells. In the upper set of panels, the absence of KCNQ1 marks the $Nr3b2^{-/-}$ marginal cells. In both the $Nr3b2^{CKO/-}$;*Nestin-cre* mosaic stria (central panels) and the $Nr3b2^{CKO/-}$;*Sox2-cre* stria (right panels), Pendrin expression in $Nr3b2^{-/-}$ marginal cells declines across the stria; the highest expression is near the spiral prominence (bottom), and the lowest expression is near the insertion of Reissner's membrane (top). Among adjacent $Nr3b2^{-/-}$ marginal cells, Pendrin expression levels vary markedly (insets). In the lower set of panels, filamentous actin is visualized with phalloidin in the same three flatmounts. Dense subcortical actin filaments are seen in WT, but not in $Nr3b2^{-/-}$, marginal cells. In the WT stria vascularis, there is some intermingling of cells at the boundary between the central zone of KCNQ1-expressing marginal cells and the flanking zones of Pendrin-expressing cells (see enlarged region, left panels). The vertical brackets to the right of the panels demarcate the extent of the stria vascularis. Asterisks indicate tissue lost during dissection.

Scale bars for all panels are 40 μm.

neurons. Among these, *Math1* is required in postmitotic hair cell precursors for the acquisition of their correct fates within the epithelial primordium (Bermingham et al., 1999; Chen et al., 2002; Woods et al., 2004), and *Brn3c* and *Gfi1* are required for the full differentiation and survival of committed hair cells (Xiang et al., 1998; Wallis et al., 2003). In contrast to the progress being made on transcription factors in early inner-ear and sensory hair cell development, virtually nothing is known about the transcriptional programs that divide the inner ear into its many precisely localized and differentiated nonsensory epithelia.

Within the cochlea, at least ten morphologically distinct epithelial cell types line the scala media (Santi, 1988). The

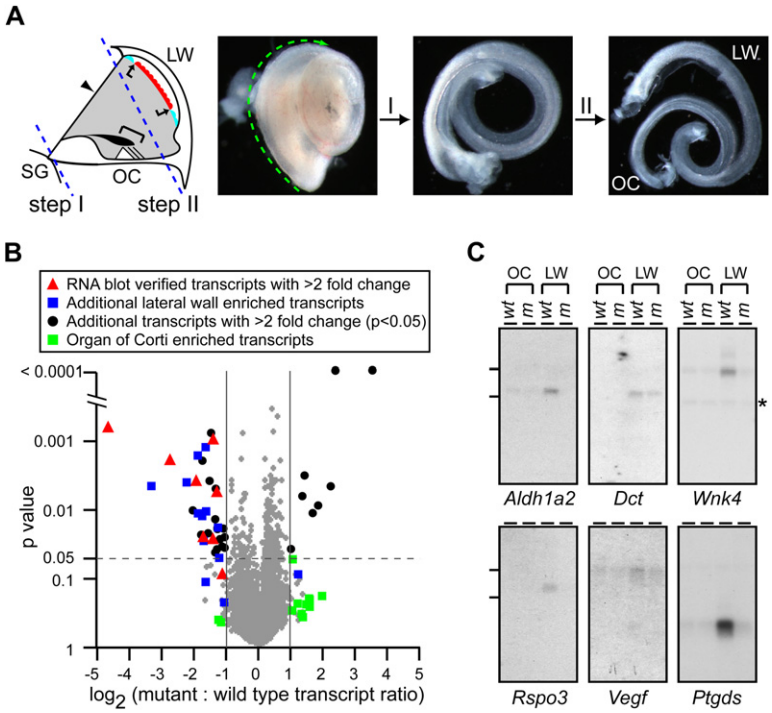

Figure 7. Comprehensive Identification of Stria Vascularis Transcripts that Change in Abundance with Loss of *Nr3b2*

(A) Dissection of the P3–P5 cochlea for microarray and northern blot hybridization. The schematic cross-section (left) and photographs (right) show the two-step dissection. In step I, the organ of Corti (OC) and lateral wall (LW) were peeled away from the spiral ganglion (SG), and in step II the lateral wall was peeled away from the organ of Corti. The lateral wall fraction contains the spiral ligament, outer sulcus, and stria vascularis. Green dashed arrow, the direction in which the dissection proceeds, from base to apex.

(B) Results of three independent dissections and microarray hybridizations with P3–P5 lateral wall RNA (20 inner ears per sample). The data are shown as a scatterplot of the abundance ratio of *Nr3b2*$^{CKO/-}$*;Sox2-cre*:WT transcripts (horizontal axis) versus the P value for each abundance ratio (vertical axis). To assess the accuracy of the dissection, transcripts from WT organ of Corti and WT lateral wall were compared by microarray hybridization (data not shown); transcripts showing >4-fold enrichment in the organ of Corti were subsequently used to monitor contamination of lateral wall preparations with tissue from the organ of Corti (green squares). Red triangles indicate transcripts for which the decrease in abundance in the *Nr3b2*$^{CKO/-}$*;Sox2-cre* lateral wall was tested by northern blot; in every case, the decrease was verified. Blue squares indicate additional lateral wall-specific transcripts, as determined by WT lateral wall versus WT organ of Corti microarray hybridization. Black circles indicate additional transcripts with >2-fold change in abundance and a P value < 0.05. For those transcripts with multiple entries in the Affymetrix spreadsheet, we have plotted only the entry with the smallest P value. See Table S1 for further details.

(C) Northern blot of P3–P5 organ of Corti (OC) and lateral wall (LW) RNA from WT and *Nr3b2*$^{CKO/-}$*;Sox2-cre* (m) with six transcripts identified by microarray hybridization as being reduced in the *Nr3b2*$^{CKO/-}$*;Sox2-cre* lateral wall. A reduction in abundance is confirmed in all cases (see also Figure 3). The mobilities of 18S and 28S rRNAs are indicated by lines to the left of the blots; the asterisk to the right of the *Wnk4* blot indicates residual hybridization from an earlier probe. *Aldhla2*, *aldehyde dehydrogenase family 1*, *subfamily A2*; *Dct*, *L-dopachrome tautomerase*; *Wnk4*, *lysine-deficient protein kinase 4*; *Rspo3*, *R-spondin 3 homolog*; *Vegf*, *vascular endothelial growth factor*; *Ptgds*, *prostaglandin D2 synthase*. Dct and Vegf show less than a 2-fold change by microarray hybridization (see Table S1). Ethidium bromide staining and *Gapdh* hybridization indicate equal RNA loading in the four wells (see Figure 3).

Nr3b2 mutant phenotype shows that a single transcription factor is devoted to the correct differentiation of one of these epithelial types, suggesting that many more as-yet-unidentified transcription factors function in the differentiation of other types. It is particularly intriguing that the *Nr3b2* mutant phenotype involves not a loss of strial marginal cells or vestibular dark cells, but instead a partial transformation of these cells toward the fate of their immediate neighbors, the Pendrin-expressing epithelial cells (Figure 8). In each inner-ear location where *Nr3b2*-expressing epithelial cells are found—the stria vascularis, the ampulla, the utricle, and the common crus (the fusion point of the posterior and superior semicircular canals)—the immediately adjacent epithelial cells express Pendrin. These two cell types thus appear to constitute a side-by-side epithelial module for potassium secretion and bicarbonate uptake. In this context, it is interesting that in Pendrin knockout (*Slc26a4*$^{-/-}$) mice there is a secondary loss of KCNJ10 channels from intermediate cells in the adjacent stria vascularis (Wangemann et al., 2004, 2007).

Among *Nr3b2*$^{-/-}$ marginal cells, the change in cell fate toward that of the neighboring Pendrin-expressing cells is uniform and complete when assessed by expression of the sc-20475 antigen, but it is incomplete in the ampulla and heterogeneous in the stria vascularis when assessed by expression of Pendrin. It is also intriguing that there is an asymmetry in the density of Pendrin-expressing marginal cells across the *Nr3b2*$^{-/-}$ stria vascularis (a pattern seen in both the mosaic and uniformly mutant situations); the largest number of transformed marginal cells are in the regions closest to the spiral prominence. By analogy with the mechanisms of cell fate specification along the dorsoventral axis of the spinal cord (Edlund and Jessell, 1999), this finding suggests that distinct epithelial cell types in the inner ear could be specified by local morphogen gradients.

A close relationship is also seen between *Nr3b2*-expressing epithelial cells and their immediate subepithelial neighbors, which invariably consist of pigmented neural crest-derived cells. At present, the molecular basis of communication among stria vascularis cell types is unknown. We speculate that some of this communication—for example, the signal that induces downregulation of KCNJ10 potassium channels in intermediate cells that

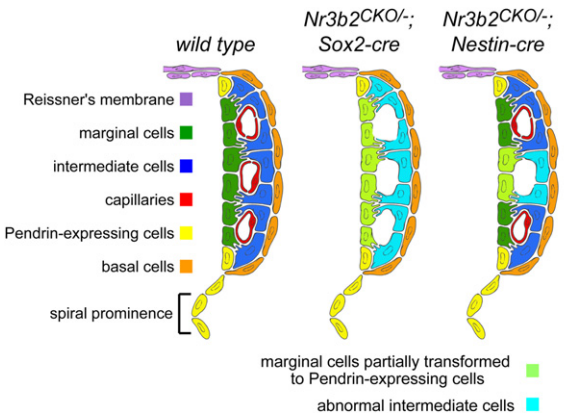

Figure 8. Schematic of the Principal Cell Types and Their Relationships in WT, *Nr3b2*$^{CKO/-}$;*Sox2-cre*, and *Nr3b2*$^{CKO/-}$;*Nestin-cre* Mosaic Stria Vascularis

In WT (left), Pendrin-expressing cells (yellow) flank a central monolayer of marginal cells (green), and capillaries (red) course between interdigitating marginal and intermediate cells (blue). In the *Nr3b2*$^{CKO/-}$;*Sox2-cre* stria vascularis (center), the capillaries are lost, marginal cells are partially transformed to Pendrin-expressing cells, and intermediate cells alter their patterns of gene expression. Each of these transformations also occurs locally in or adjacent to *Nr3b2*$^{-/-}$ marginal cells in the mosaic *Nr3b2*$^{CKO/-}$;*Nestin-cre* stria vascularis.

contact *Nr3b2*$^{-/-}$ marginal cells—could represent a normal homeostatic pathway that regulates endolymph production and composition.

NR3B2 and the Role of Nuclear Receptors in Cell Fate Decisions

The mouse genome encodes 49 nuclear receptors, and their functions can be roughly divided into the regulation of (1) reproduction, development, and growth, and (2) nutrient uptake, metabolism, and excretion (Bookout et al., 2006). The function of NR3B2 in placental (Luo et al., 1997), germ cell (Mitsunaga et al., 2004), and inner-ear development falls within the first of these categories. The distinctive feature of NR3B2 function in the inner ear is that it regulates a decision between two similar cell fates. Conceptually similar functions have been described for several nuclear receptors in the retina. NR2E3, an orphan nuclear receptor expressed in postmitotic rod photoreceptors, is required to suppress a large number of cone-specific genes in rods (Chen et al., 2005; Corbo and Cepko, 2005; Peng et al., 2005), and in its absence there is a partial conversion of all rods into a cone cell fate. In cone photoreceptor development, thyroid hormone and the thyroid hormone receptor β2 (TR-β2) are required for the correct differentiation of middle-wavelength sensitive cones: in the absence of thyroid hormone action, these cells are converted to short-wave sensitive cones (Ng et al., 2001; Roberts et al., 2006). Additionally, retinoid X receptor γ (RXR-γ), a potential dimerization partner of TR-β2, is required in middle-wave cones for the suppression of short-wave opsin expression, but not for the activation of middle-wave opsin (Roberts et al., 2005), and retinoid-related orphan receptor β (ROR-β) is required for short-wave opsin expression in short-wave cones (Srinivas et al., 2006). These precedents in the retina suggest that a systematic and detailed examination of the patterns of inner-ear expression for all 49 nuclear receptors might reveal additional candidates for developmental regulators of cell fate. Consistent with this idea, it is known that thyroid hormone receptors are required for normal inner-ear development (Rusch et al., 2001).

With respect to the action of NR3B2 in inner-ear development, a number of questions remain. Are there endogenous ligands and dimerization partners for NR3B2? Which genes are direct and which are indirect targets of NR3B2 regulation? What regulates the expression of the *Nr3b2* gene? With respect to the last of these questions, the unaltered abundance of transcripts from the exon 2-deleted *Nr3b2* allele in *Nr3b2*$^{-/-}$ marginal cells implies that *Nr3b2* expression is neither maintained by positive autoregulation nor repressed by negative autoregulation.

Finally, we note that *Nr3b2* is expressed in postmitotic rod photoreceptors with essentially the same time course as *Nr2e3*. However, by immunostaining with a variety of rod- and cone-specific markers, we see no evidence for alterations in cell fate, viability, or structure in the *Nr3b2*$^{-/-}$ retina (data not shown). Thus, if NR3B2 has a role in retinal development, it is either quite subtle or largely obscured by redundancy with other transcription factors.

Implications for Inner-Ear Disease

The inner-ear defects caused by loss of *Nr3b2* suggest that this gene should be considered a candidate for hereditary hearing loss in humans. We note, however, that the essential role of *Nr3b2* in mouse placental development, if conserved across species, suggests that inner-ear defects would only be found in humans in the context of allelic combinations that partially preserve *Nr3b2* function. Of potentially more general significance to the identification of candidate genes for hereditary hearing loss, the microarray hybridization of dissected WT and *Nr3b2*$^{-/-}$ lateral wall has revealed a set of differentially regulated genes, several of which are already known to be essential for endolymph homeostasis.

In addition to providing candidate genes that may be relevant to inherited inner-ear disorders, NR3B2 and some of the proteins that are encoded by NR3B2-regulated genes represent potential targets for small-molecule therapies aimed at altering endolymph homeostasis. NR3B2 is an especially interesting candidate because partial blockade of NR3B2 action would be predicted to decrease endolymph production, an effect that could be efficacious in the context of Meniere's disease, which, as noted in the Introduction, is associated with excessive endolymph. Systemic treatment with an NR3B2 antagonist might have minimal side effects, because in *Nr3b2*$^{CKO/-}$;*Sox2-cre* mice the complete loss of NR3B2 in all somatic tissues has no obvious effect on overall health aside from the inner-ear defect. In contrast, targeting individual channels or transporters involved in

endolymph production might result in substantial systemic toxicity because these proteins play important roles in multiple other organs, including the heart and kidneys. At present, the only well-characterized NR3B2 ligands are diethylstilbesterol and 4-hydroxytamoxifen, but neither are specific for NR3B2, and each interacts with NR3B2 with relatively low (micromolar) affinity (Tremblay et al., 2001a, 2001b; Horard and Vanacker, 2003; Ariazi and Jordan, 2006). The synthesis of new ligands with greater affinity and specificity will be required to evaluate NR3B2 as a potential drug target for disorders of inner-ear fluid homeostasis.

EXPERIMENTAL PROCEDURES

Production and Breeding of *Nr3b2*^{CKO} Mice

To generate a conditional allele of *Nr3b2*, two *loxP* sites (5′-ATAAC TTCGTATAGCATACATTATACGAAGTTAT-3′) were placed in introns 184 bp upstream and 123 bp downstream, respectively, of the second *Nr3b2* exon. A neomycin selection marker under the control of the *phosphoglycerate kinase* (*PGK*) promoter was flanked by two FRT sites (5′-GAAGTTCCTATTCTCTAGAAAGTATAGGAACTTC-3′) and placed immediately downstream of the 3′ *loxP* site. 129/SvJ embryonic stem (ES) cells were used for gene targeting and screened by Southern blot. ES cell clones with the targeted *Nr3b2* allele and normal karyotype were injected into C57BL/6 blastocysts. The resulting chimeric male mice were mated to C57BL/6 females and germline transmission of the *Nr3b2* conditional allele containing the neomycin selection marker (*Nr3b2*$^{CKO+neo}$) was confirmed by Southern blot. The neomycin selection cassette was excised by crossing to mice constitutively expressing the Flp recombinase (Rodriguez et al., 2000), generating the *Nr3b2* conditional allele (*Nr3b2*^{CKO}). To generate a germline *Nr3b2* null allele (*Nr3b2*$^{-}$), mice carrying either the *Nr3b2*$^{CKO+neo}$ allele (for the *Nestin-cre* mosaic experiments) or the *Nr3b2*^{CKO} allele (for the *Sox2-cre* experiments) were mated to female *Sox2-cre* transgenic mice (Hayashi et al., 2003) (*Tg(Sox2-cre)1Amc/J*; The Jackson Laboratory, Bar Harbor, ME). *Nr3b2* mosaic mice were produced by crossing in a *Nestin-cre* transgene (Tronche et al., 1999) (*B6.Cg-Tg(Nes-cre)1Kln/J*; The Jackson Laboratory, Bar Harbor, ME). To generate progeny with genotypes *Nr3b2*$^{CKO/-}$*;Sox2-cre* or *Nr3b2*$^{CKO/-}$*;Nestin-cre* as well as phenotypically WT littermates, the following crosses were performed: *Nr3b2*$^{CKO/-}$*;Sox2-cre* (male) × *Nr3b2*$^{CKO/CKO}$ (female) or *Nr3b2*$^{CKO/-}$*;Nestin-cre* (male) × *Nr3b2*$^{CKO/CKO}$ (female). In each of these crosses, the males were heterozygous for the *cre* transgene.

Antibodies

Rabbit polyclonal antibodies against the mouse *Nr3b2* linker region (amino acids 186–237) were generated by immunization with a T7 gene 10 fusion protein (Studier et al., 1990) and affinity purified with an immobilized glutathione S-transferase (GST) fusion protein carrying the same *Nr3b2* sequence. Other antibodies used were: goat anti-KCNQ1 (sc-10646, Santa Cruz), rabbit anti-SLC12A2 (Ab3560P, Chemicon), rabbit anti-KCNJ10 (APC-035, Alomone), rabbit anti-Pendrin (a gift of Soren Nielsen) (Kim et al., 2002), goat anti-WNK4 (which instead recognizes a cytosolic antigen in Pendrin-expressing cells; sc-20475, Santa Cruz), and rat anti-PECAM (557355, Chemicon). Texas red-conjugated GS-lectin (I-21413) and Alexa 647-conjugated phalloidin (A22287) were purchased from Molecular Probes.

Auditory Brainstem Responses

Nr3b2$^{CKO/-}$*;Sox2-cre* and *Nr3b2*$^{CKO/-}$*;Nestin-cre* as well as WT littermate controls between 1 and 3 months of age were anesthetized with a 100 mg/kg mixture of Ketamine (8 mg/ml) and Xylazine (1.2 mg/ml). When the paw pinch reflex disappeared, three electrodes were placed subcutaneously on the vertex of the head, in the postauricular region, and in the dorsum of the neck. Broadband clicks (100 μs duration) were presented binaurally by using a Tucker Davis System 3 (Tucker Davis Technologies, Alachua, FL), and the auditory brainstem responses (ABRs) were recorded for 30 ms with a Crown Amplifier (Crown International, Elkhart, IN). Broadband clicks were presented at a starting intensity of 10 dB SPL, with intensity increasing in increments of 10 dB SPL up to 110 dB SPL. At each intensity, the ABR was determined by averaging 500 responses. Thresholds were calculated by comparing the signal (3–8 ms after sound presentation) with the noise (25–30 ms after sound presentation). The threshold was defined as the point at which the signal rose two standard deviations above the noise.

Tissue Preparation and Immunohistochemistry

Dissected mouse inner ears were punctured at both the oval and round windows and were fixed with 4% paraformaldehyde in PBS for 15 min on ice. For animals older than P5, inner ears were decalcified in PBS with 0.2 M ethylenediaminetetraacetic acid (EDTA) for 1–2 days at 4°C. The fixed inner ears were cryoprotected in PBS with 20% sucrose at 4°C overnight and then embedded in Optimal Cutting Temperature Compound (OCT; Tissue-Tek, Tokyo, Japan). Immunostaining of frozen sections was carried out essentially as described (Chen et al., 2005), except that normal donkey serum was used for blocking when using goat primary antibodies. For whole-mount immunostaining, inner ears were fixed and decalcified as described above. The bony sheath and the central modiolus were removed from the cochlea, and the lateral walls were blunt dissected but were allowed to remain attached to the organ of Corti at one end to facilitate visualization. After three washes in PBS, the lateral walls were incubated with blocking buffer (PBS with 5% normal goat or donkey serum and 0.3% Triton X-100), and then incubated with primary antibodies in blocking buffer at 4°C overnight. The following day, the lateral walls were washed in wash buffer (PBS with 1% Triton X-100 and 1% Tween 20) for 4 hr at room temperature and then incubated with secondary antibodies diluted in blocking buffer at 4°C overnight. The lateral walls were then washed as described above and flat mounted with the marginal cells facing up. Images were captured on a confocal microscope (LSM510; Zeiss, Oberkochen, Germany). Images for each Z stack were taken at 1 μm intervals and were projected onto the X-Y plane with no change in the maximal intensities of individual sections.

In Situ Hybridization

In situ hybridization was performed essentially as described (Schaeren-Wiemers and Gerfin-Moser, 1993). Digoxigenin-labeled riboprobes were transcribed with T7 RNA polymerase from the indicated cDNAs, which were isolated either as clones from cDNA libraries or as cloned PCR products derived from mouse inner-ear RNA. Images were captured on a Zeiss Imager Z1 microscope with Zeiss AxioVision 4.5 software.

RNA Blot and Microarray Hybridization

As illustrated in Figure 7, the organ of Corti and the lateral walls of the cochlea from ~P3 to ~P5 *Nr3b2*$^{CKO/-}$*;Sox2-cre* mice and WT littermates were microdissected. Tissues were snap frozen in dry ice, and RNA was extracted by using Trizol (Invitrogen, Carlsbad, CA) and an RNeasy kit (QIAGEN, Valencia, CA). RNA blot hybridization was performed by using standard methods with ^{32}P-labeled cDNA probes, which were isolated as described in the preceding paragraph. Lateral wall RNA from WT and *Nr3b2*$^{CKO/-}$*;Sox2-cre* mice (3 independent dissections of 20 inner ears per sample) or RNA from WT organ of Corti and WT lateral wall (1 dissection) were used in microarray experiments with mouse genome 430 2.0 microarrays (Affymetrix, Santa Clara, CA). For the triplicate lateral wall comparison, data were processed as described (Chen et al., 2005).

Supplemental Data

Supplemental Data include the results of inner-ear microarray hybridization and are available at http://www.developmentalcell.com/cgi/content/full/13/3/325/DC1/.

ACKNOWLEDGMENTS

The authors thank Hugh Cahill for performing the auditory brainstem response (ABR) measurements, Brad May and David Ryugo for providing the ABR equipment, Soren Nielsen for the gift of anti-Pendrin antibodies, Charles Hawkins for embryonic stem cell injection into embryos, Francisco Murillo for microarray hybridization, Amir Rattner for *Ednrb*$^{s-l/s-l}$ mice, Tim Phelps for drawing Figure 8, Amir Rattner for advice, and Paul Fuchs and Amir Rattner for comments on the manuscript.

Received: May 22, 2007
Revised: July 16, 2007
Accepted: July 18, 2007
Published: September 4, 2007

REFERENCES

Ando, M., and Takeuchi, S. (1999). Immunological identification of an inward rectifier K^+ channel (Kir4.1) in the intermediate cell (melanocyte) of the cochlear stria vacsularis of gerbils and rats. Cell Tissue Res. *298*, 179–183.

Anniko, M. (1988). Functional morphology of the vestibular system. In Physiology of the Ear, A.F. Jahn and J. Santos-Sacchi, eds. (New York: Raven Press), pp. 457–475.

Ariazi, E.A., and Jordan, V.C. (2006). Estrogen-related receptors as emerging targets in cancer and metabolic disorders. Curr. Top. Med. Chem. *6*, 203–215.

Bermingham, N.A., Hassan, B.A., Price, S.D., Vollrath, M.A., Ben-Arie, N., Eatock, R.A., Bellen, H.J., Lysakowski, A., and Zoghbi, H.Y. (1999). Math1: an essential gene for the generation of inner ear hair cells. Science *284*, 1837–1841.

Bookout, A.L., Jeong, Y., Downes, M., Yu, R.T., Evans, R.M., and Mangelsdorf, D.J. (2006). Anatomical profiling of nuclear receptor expression reveals a hierarchical transcriptional network. Cell *126*, 789–799.

Burton, Q., Cole, L.K., Mulheisen, M., Chang, W., and Wu, D.K. (2004). The role of Pax2 in mouse inner ear development. Dev. Biol. *272*, 161–175.

Casimiro, M.C., Knollmann, B.C., Ebert, S.N., Vary, J.C., Jr., Greene, A.E., Franz, M.R., Grinberg, A., Huang, S.P., and Pfeifer, K. (2001). Targeted disruption of the Kcnq1 gene produces a mouse model of Jervell and Lange-Nielsen Syndrome. Proc. Natl. Acad. Sci. USA *98*, 2526–2531.

Chen, J., Rattner, A., and Nathans, J. (2005). The rod photoreceptor-specific nuclear receptor Nr2e3 represses transcription of multiple cone-specific genes. J. Neurosci. *25*, 118–129.

Chen, P., Johnson, J.E., Zoghbi, H.Y., and Segil, N. (2002). The role of Math1 in inner ear development: uncoupling the establishment of the sensory primordium from hair cell fate determination. Development *129*, 2495–2505.

Corbo, J.C., and Cepko, C.L. (2005). A hybrid photoreceptor expressing both rod and cone genes in a mouse model of enhanced S-cone syndrome. PLoS Genet. *1*, e11.

Delpire, E., Lu, J., England, R., Dull, C., and Thorne, T. (1999). Deafness and imbalance associated with inactivation of the secretory Na-K-2Cl co-transporter. Nat. Genet. *22*, 192–195.

Dixon, M.J., Gazzard, J., Chaudhry, S.S., Sampson, N., Schulte, B.A., and Steel, K.P. (1999). Mutation of the Na-K-Cl co-transporter gene Slc12a2 results in deafness in mice. Hum. Mol. Genet. *8*, 1579–1584.

Edlund, T., and Jessell, T.M. (1999). Progression from extrinsic to intrinsic signaling in cell fate specification: a view from the nervous system. Cell *96*, 211–224.

Everett, L.A., Glaser, B., Beck, J.C., Idol, J.R., Buchs, A., Heyman, M., Adawi, F., Hazani, E., Nassir, E., Baxevanis, A.D., et al. (1997). Pendred syndrome is caused by mutations in a putative sulphate transporter gene (PDS). Nat. Genet. *17*, 411–422.

Flagella, M., Clarke, L.L., Miller, M.L., Erway, L.C., Giannella, R.A., Andringa, A., Gawenis, L.R., Kramer, J., Duffy, J.J., Doetschman, T., et al. (1999). Mice lacking the basolateral Na-K-2Cl cotransporter have impaired epithelial chloride secretion and are profoundly deaf. J. Biol. Chem. *274*, 26946–26955.

Friedmann, I., Fraser, G.R., and Froggatt, P. (1966). Pathology of the ear in the cardioauditory syndrome of Jervell and Lange-Nielson (recessive deafness with electrocardiographic abnormalities). J. Laryngol. Otol. *80*, 451–470.

Gates, G.A. (2006). Meniere's disease. J. Am. Acad. Audiol. *17*, 16–26.

Hayashi, S., Lewis, P., Pevny, L., and McMahon, A.P. (2002). Efficient gene modulation in mouse epiblast using a Sox2Cre transgenic mouse strain. Gene Expr. Patterns *2*, 93–97.

Hayashi, S., Tenzen, T., and McMahon, A.P. (2003). Maternal inheritance of Cre activity in a Sox2Cre deleter strain. Genesis *37*, 51–53.

Horard, B., and Vanacker, J.M. (2003). Estrogen receptor-related receptors: orphan receptors desperately seeking a ligand. J. Mol. Endocrinol. *31*, 349–357.

Hudspeth, A.J. (2001). How the ear's works work: mechanoelectrical transduction and amplification by hair cells of the internal ear. Harvey Lect. *97*, 41–54.

Hulander, M., Wurst, W., Carlsson, P., and Enerback, S. (1998). The winged helix transcription factor Fkh10 is required for normal development of the inner ear. Nat. Genet. *20*, 374–376.

Kahle, K.T., Gimenez, I., Hassan, H., Wilson, F.H., Wong, R.D., Forbush, B., Aronson, P.S., and Lifton, R.P. (2004). WNK4 regulates apical and basolateral Cl^- flux in extrarenal epithelia. Proc. Natl. Acad. Sci. USA *101*, 2064–2069.

Kim, Y.-H., Kwon, T.-H., Frische, S., Kim, J., Tisher, C.C., Madsen, K.M., and Nielsen, S. (2002). Immunocytochemical localization of pendrin in intercalated cell subtypes in rat and mouse kidney. Am. J. Physiol. Renal Physiol. *283*, F744–F754.

Lane, P.W. (1966). Association of megacolon with two recessive spotting genes in the mouse. J. Hered. *57*, 29–31.

Lee, M.P., Ravenel, J.D., Hu, R.J., Lustig, L.R., Tomaselli, G., Berger, R.D., Brandenburg, S.A., Litzi, T.J., Bunton, T.E., Limb, C., et al. (2000). Targeted disruption of the Kvlqt1 gene causes deafness and gastric hyperplasia in mice. J. Clin. Invest. *106*, 1447–1455.

Letts, V.A., Valenzuela, A., Dunbar, C., Zheng, Q.Y., Johnson, K.R., and Frankel, W.N. (2000). A new spontaneous mouse mutation in the Kcne1 gene. Mamm. Genome *11*, 831–835.

Luo, J., Sladek, R., Bader, J.A., Matthyssen, A., Rossant, J., and Giguere, V. (1997). Placental abnormalities in mouse embryos lacking the orphan nuclear receptor ERR-β. Nature *388*, 778–782.

Marcus, D.C., Wu, T., Wangemann, P., and Kofuji, P. (2002). KCNJ10 (Kir4.1) potassium channel knockout abolishes endocochlear potential. Am. J. Physiol. Cell Physiol. *282*, C403–C407.

Mitsunaga, K., Araki, K., Mizusaki, H., Morohashi, K., Haruna, K., Nakagata, N., Giguere, V., Yamamura, K., and Abe, K. (2004). Loss of PGC-specific expression of the orphan nuclear receptor ERR-β results in reduction of germ cell number in mouse embryos. Mech. Dev. *121*, 237–246.

Moraes, F., Novoa, A., Jerome-Majewska, L.A., Papaioannou, V.E., and Mallo, M. (2005). Tbx1 is required for proper neural crest migration and to stabilize spatial patterns during middle and inner ear development. Mech. Dev. *122*, 199–212.

Ng, L., Hurley, J.B., Dierks, B., Srinivas, M., Salto, C., Vennstrom, B., Reh, T.A., and Forrest, D. (2001). A thyroid hormone receptor that is required for the development of green cone photoreceptors. Nat. Genet. *27*, 94–98.

Ozaki, H., Nakamura, K., Funahashi, J., Ikeda, K., Yamada, G., Tokano, H., Okamura, H.O., Kitamura, K., Muto, S., Kotaki, H., Sudo,

K., Horai, R., Iwakura, Y., and Kawakami, K. (2004). Six1 controls patterning of the mouse otic vesicle. Development *131*, 551–562.

Paparella, M.M., and Djalilian, H.R. (2002). Etiology, pathophysiology of symptoms, and pathogenesis of Meniere's disease. Otolaryngol. Clin. North Am. *35*, 529–545.

Peng, G.H., Ahmad, O., Ahmad, F., Liu, J., and Chen, S. (2005). The photoreceptor-specific nuclear receptor Nr2e3 interacts with Crx and exerts opposing effects on the transcription of rod versus cone genes. Hum. Mol. Genet. *14*, 747–764.

Peters, T.A., Monnens, L.A., Cremers, C.W., and Curfs, J.H. (2004). Genetic disorders of transporters/channels in the inner ear and their relation to the kidney. Pediatr. Nephrol. *19*, 1194–1201.

Petit, C., Levilliers, J., Marlin, S., and Hardelin, J.P. (2001). Hereditary hearing loss. In The Metabolic and Molecular Bases of Inherited Diseases, Eighth Edition, C.R. Scriver, A.L. Beaudet, W.S. Sly, and D. Valle, eds. (New York: McGraw-Hill), pp. 6281–6328.

Roberts, M.R., Hendrickson, A., McGuire, C.R., and Reh, T.A. (2005). Retinoid X receptor (γ) is necessary to establish the S-opsin gradient in cone photoreceptors of the developing mouse retina. Invest. Ophthalmol. Vis. Sci. *46*, 2897–2904.

Roberts, M.R., Srinivas, M., Forrest, D., Morreale de Escobar, G., and Reh, T.A. (2006). Making the gradient: thyroid hormone regulates cone opsin expression in the developing mouse retina. Proc. Natl. Acad. Sci. USA *103*, 6218–6223.

Rodriguez, C.I., Buchholz, F., Galloway, J., Sequerra, R., Kasper, J., Ayala, R., Stewart, A.F., and Dymecki, S.M. (2000). High-efficiency deleter mice show that FLPe is an alternative to Cre-loxP. Nat. Genet. *25*, 139–140.

Rusch, A., Ng, L., Goodyear, R., Oliver, D., Lisoukov, I., Vennstrom, B., Richardson, G., Kelley, M.W., and Forrest, D. (2001). Retardation of cochlear maturation and impaired hair cell function caused by deletion of all known thyroid hormone receptors. J. Neurosci. *21*, 9792–9800.

Santi, P.A. (1988). Cochlear microanatomy and ultrastructure. In Physiology of the Ear, A.F. Jahn and J. Santos-Sacchi, eds. (New York: Raven Press), pp. 173–199.

Schaeren-Wiemers, N., and Gerfin-Moser, A. (1993). A single protocol to detect transcripts of various types and expression levels in neural tissue and cultured cells: in situ hybridization using digoxygenin-labelled cRNA probes. Histochemistry *100*, 431–440.

Schulze-Bahr, E., Wang, Q., Wedekind, H., Haverkamp, W., Chen, Q., Sun, Y., Rubie, C., Hordt, M., Towbin, J.A., Borggrefe, M., et al. (1997). KCNE1 mutations cause Jervell and Lange-Nielsen syndrome. Nat. Genet. *17*, 267–268.

Srinivas, M., Ng, L., Liu, H., Jia, L., and Forrest, D. (2006). Activation of the blue opsin gene in cone photoreceptor development by retinoid-related orphan receptor β. Mol. Endocrinol. *20*, 1728–1741.

Steel, K.P. (1995). Inherited hearing defects in mice. Annu. Rev. Genet. *29*, 675–701.

Studier, F.W., Rosenberg, A.H., Dun, J.J., and Dubendorf, J.W. (1990). Use of T7 RNA polymerase to direct expression of cloned genes. Methods Enzymol. *185*, 60–89.

Tachibana, M., Kobayashi, Y., and Matsushima, Y. (2003). Mouse models of four types of Waardendurg syndrome. Pigment Cell Res. *16*, 448–454.

Tremblay, G.B., Bergeron, D., and Giguere, V. (2001a). 4-Hydroxytamoxifen is an isoform-specific inhibitor of orphan estrogen-receptor-related (ERR) nuclear receptors β and γ. Endocrinology *142*, 4572–4575.

Tremblay, G.B., Kunath, T., Bergeron, D., Lapointe, L., Champigny, C., Bader, J.A., Rossant, J., and Giguere, V. (2001b). Diethylstilbestrol regulates trophoblast stem cell differentiation as a ligand of orphan nuclear receptor ERR β. Genes Dev. *15*, 833–838.

Tronche, F., Kellendonk, C., Kretz, O., Gass, P., Anlag, K., Orban, P.C., Bock, R., Klein, R., and Schutz, G. (1999). Disruption of the glucocorticoid receptor gene in the nervous system results in reduced anxiety. Nat. Genet. *23*, 99–103.

Vetter, D.E., Mann, J.R., Wangemann, P., Liu, J., McLaughlin, K.J., Lesage, F., Marcus, D.C., Lazdunski, M., Heinemann, S.F., and Barhanin, J. (1996). Inner ear defects induced by null mutation of the isk gene. Neuron *17*, 1251–1264.

Von Bekesy, G. (1952). Resting potentials inside the cochlear partition of the guinea pig. Nature *169*, 241–242.

Wallis, D., Hamblen, M., Zhou, Y., Venken, K.J., Schumacher, A., Grimes, H.L., Zoghbi, H.Y., Orkin, S.H., and Bellen, H.J. (2003). The zinc finger transcription factor Gfi1, implicated in lymphomagenesis, is required for inner ear hair cell differentiation and survival. Development *130*, 221–232.

Wang, Z., Li, H., Moss, A.J., Robinson, J., Zareba, W., Knilans, T., Bowles, N.E., and Towbin, J.A. (2002). Compound heterozygous mutations in KvLQT1 cause Jervell and Lange-Nielson syndrome. Mol. Genet. Metab. *75*, 308–316.

Wangemann, P. (1995). Comparison of ion transport mechanisms between vestibular dark cells and strial marginal cells. Hear. Res. *90*, 149–157.

Wangemann, P. (2006). Supporting sensory transduction: cochlear fluid homeostasis and the endocochlear potential. J. Physiol. *576*, 11–21.

Wangemann, P., Itza, E.M., Albrecht, B., Wu, T., Jabba, S.V., Maganti, R.J., Lee, J.H., Everett, L.A., Wall, S.M., Royaux, I.E., et al. (2004). Loss of KCNJ10 protein abolishes endocochlear potential and causes deafness in Pendred syndrome mouse. BMC Med. *2*, 30.

Wangemann, P., Nakaya, K., Wu, T., Maganti, R.J., Itza, E.M., Sanneman, J.D., Harbidge, D.G., Billings, S., and Marcus, D.C. (2007). Loss of cochlear HCO_3^- secretion causes deafness via endolymphatic acidification and inhibition of Ca^{2+} resorption in a Pendred syndrome mouse model. Am. J. Physiol. Renal Physiol. *292*, F1345–F1353.

Woods, C., Montcouquiol, M., and Kelley, M.W. (2004). Math1 regulates development of the sensory epithelium in the mammalian cochlea. Nat. Neurosci. *7*, 1310–1318.

Xiang, M., Gao, W.Q., Hasson, T., and Shin, J.J. (1998). Requirement for Brn-3c in maturation and survival, but not in fate determination of inner ear hair cells. Development *125*, 3935–3946.

Zheng, W., Huang, L., Wei, Z.B., Silvius, D., Tang, B., and Xu, P.X. (2003). The role of Six1 in mammalian auditory system development. Development *130*, 3989–4000.

Zou, D., Silvius, D., Rodrigo-Blomqvist, S., Enerback, S., and Xu, P.X. (2006). Eya1 regulates the growth of otic epithelium and interacts with Pax2 during the development of all sensory areas in the inner ear. Dev. Biol. *298*, 430–441.

Accession Numbers

Microarray hybridization data have been deposited in the GEO database with accession code GSE8434.